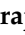


Article

Experimental Study on the Natural Dynamic Characteristics of Steel-Framed Modular Structures

Mostafa Farajian ^{1,*}, Pejman Sharafi ¹ , Ali Bigdeli ², Hadi Eslamnia ³ and Payam Rahnamayezekavat ¹

¹ Centre for Infrastructure Engineering, School of Engineering, Design and Built Environment, Western Sydney University, Penrith 2747, Australia; p.sharafi@westernsydney.edu.au (P.S.); p.zekavat@westernsydney.edu.au (P.R.)

² Department of Civil and Environmental Engineering, Tarbiat Modares University, Tehran 14115-111, Iran; alibigdeli@modares.ac.ir

³ Department of Civil and Environmental Engineering, Amirkabir University of Technology, Tehran 15875-4413, Iran; h.eslamnia@aut.ac.ir

* Correspondence: 19918671@student.westernsydney.edu.au

Abstract: Corner-supported modular structures are made of repetitive prefurnished, prefabricated modular units, which are fabricated in a factory and transported to the site of a building to form a permanent building block. The modular units are then tied together through the use of so-called inter-modular connections, or inter-connections, which form a different configuration at joints compared to conventional steel structures. The presence of inter-connections in these structures, in addition to beam-to-column connections or intra-connections, may change their dynamic characteristics, including natural frequencies, mode shapes, and damping ratios. This paper aims to investigate the dynamic characteristics of a modular building through the use of operational modal analysis (OMA). A half-scaled three-storey modular structure, designed and instrumented with highly sensitive accelerometers, was experimentally tested under pure and randomly generated vibrations. The time history of the response acceleration of the structure was recorded using a data acquisition system. Different output-only techniques of OMA, based on both frequency and time domains, were employed to analyse the recorded response acceleration of the structure and extract the natural frequencies, mode shapes, and damping ratios. These techniques are peak picking (PP), enhanced frequency-domain decomposition (EFDD), and stochastic subspace identification (SSI). The outcomes in this paper can be used for further research on the development of an experimental formula for the design of multistorey modular buildings against lateral loads.

Keywords: modular structures; natural frequency; experimental study; inter-connection; damping ratio; mode shape; operational modal analysis



Citation: Farajian, M.; Sharafi, P.; Bigdeli, A.; Eslamnia, H.; Rahnamayezekavat, P. Experimental Study on the Natural Dynamic Characteristics of Steel-Framed Modular Structures. *Buildings* **2022**, *12*, 587. <https://doi.org/10.3390/buildings12050587>

Received: 7 April 2022

Accepted: 29 April 2022

Published: 2 May 2022

Publisher's Note: MDPI stays neutral with regard to jurisdictional claims in published maps and institutional affiliations.



Copyright: © 2022 by the authors. Licensee MDPI, Basel, Switzerland. This article is an open access article distributed under the terms and conditions of the Creative Commons Attribution (CC BY) license (<https://creativecommons.org/licenses/by/4.0/>).

1. Introduction

Modular construction is a relatively new type of construction method as an alternative approach to the traditional construction method [1]. Modules are fabricated and fully equipped in factories, transported to the site of a building, and connected together at their corners through the use of inter-modular connections or inter-connections to build a permanent structure. Modular construction offers some advantages, such as improving construction quality and reducing on-site construction time, labour effort, and material wastage [2]. Due to the ease of installation and production of modular units, the application of modular construction has recently been promoted to build different types of structures, such as residential buildings, dormitories, hotels, hospitals, and schools [3].

Inter-connections in corner-supported steel modular buildings play a significant role in the integrity and stability of these structures. Moreover, they provide pathways to transfer induced gravity and lateral forces from different elements, such as beams and columns, to the foundation and ground. The introduction of inter-connections to corner-supported

modular buildings changes the boundary conditions of columns and the configuration of joints compared to conventional steel structures [4]. That is because, while in conventional structures, each joint comprises a continuous column and two beams connected by beam-to-column connections, each joint in a corner-supported modular building is formed by up to eight discontinuous columns and sixteen beams that are connected by beam-to-column connections or intra-connections, in addition to inter-connections [4]. The lack of continuity in the joints of a modular structure will lead to changes in the stiffness and dynamic properties of the structure, affecting its behaviour and performance against gravity and lateral actions [4,5]. Therefore, having comprehensive knowledge on the influence of inter-connections on the static and dynamic behaviours of modular buildings is indispensable in their design process. Figure 1 compares the details of a joint in a conventional steel building with that in a corner-supported modular steel building.

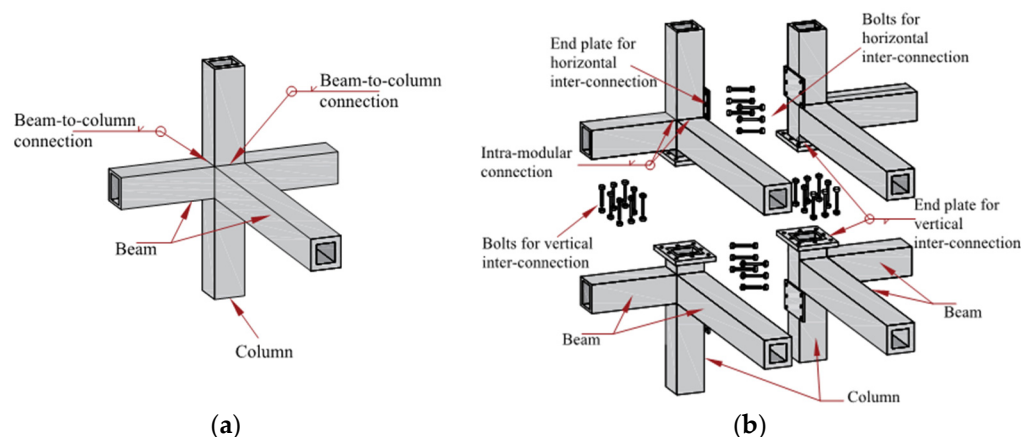


Figure 1. Details of a joint in (a) conventional (b) corner-supported modular structures.

Despite the fact that the modular construction method provides many advantages, structural engineers still rely on the available standards and codes for the design of conventional buildings in the design procedure of a modular structure due to the lack of sufficient experimental tests and numerical simulations on corner-supported modular structures. While the optimal design of conventional structures has been studied extensively [6–8], limited works have been conducted on the optimum design of multistorey modular buildings [9,10]. The literature on this topic mainly focuses on the development of inter-connections, in which a wide variety of inter-connections have been proposed as horizontal and/or vertical inter-connections. Chen et al. [11] proposed an innovative inter-connection for modular structures, in which horizontal and vertical connectivity is provided through the use of an intermediate plug-in device and a beam-to-beam bolt system. Experimental tests and numerical simulations indicated that the deformation capacity of the connection was significantly affected by the stiffness of the connection at both floor and ceiling beams. Further investigation conducted by Chen et al. [12] indicated that adding stiffeners to the inter-connections significantly increased the stiffness and load-bearing capacity of the connection. On the other hand, the ductility may be reduced. Sanches et al. [13] conducted experimental tests on a novel inter-connection for modular steel buildings. The inter-connection comprised a post-tensioned (PT) rod and a steel box placed between two modules. The results showed that the proposed connection had a lateral stiffness and strain distribution similar to those of on-site welding connections. Therefore, welding connections can be replaced with PT connections. The seismic performance of the ceiling-bracket-type modular joint was evaluated by Lee et al. [14]. The experimental results demonstrated that the energy dissipation capacity of the ceiling-bracket type modular joint was higher than those of other modular joints. More conducted experimental and numerical studies concentrated on the seismic behaviour of modular structures and enhancing their lateral performance [15–20]. However, when it comes to structural dynamic characteristics, such as the natural frequency, mode shape, and damping ratio, the literature is almost silent.

The dynamic characteristics of a building are key features in the analysis and design of a structure against lateral loads [21–24]. In particular, in the initial design procedure of a structure against earthquake actions, all standards and codes rely on the experimental formula to evaluate the fundamental period of the structure to determine the level of earthquake actions induced on the structure. However, relevant formulas for estimating the fundamental natural frequency of conventional structures may not be appropriate for modular buildings, mainly due to the different configurations of joints in these structures. Therefore, the study of the dynamic characteristics of modular structures is vital.

A number of studies, both numerical and experimental, on the modal analysis of conventional structures have been performed in the past. A modal analysis of a frame with semi-rigid behaviour of a beam-to-column connection was conducted by modifying the stiffness matrix of the beam element [25]. The results showed that the natural frequency of the frame increased with the decrease in the connection's stiffness. Goksu et al. [26] conducted field testing on two full-scale reinforced concrete (RC) structures to evaluate the effect of the damage level on the modal frequencies and damping ratios of the structures. They concluded that the increase in the level of damage resulted in a decrease in modal frequencies. Memari et al. [27] evaluated the dynamic characteristics of a full-scale six-storey steel frame during building construction. Sophianopoulos [28] conducted a parametric study to investigate the effect of joint flexibility on the free elastic vibration characteristics of an L-shaped steel frame. The effect of brace stiffness on the dynamic characteristics of a steel frame was studied by Turker and Bayraktar [29] through experimental tests and numerical simulations. They concluded that the natural frequencies of the structure increased when adding brace elements due to the fact that the brace elements increase the stiffness of the structure. Recently, the scanning laser Doppler vibrometer (SLLDV) system was developed and employed in vibration analysis due to the fact that it facilitates non-contact and spatially dense measurements [30]. In this method, a laser spot moves continuously on the surface of a structure, and the structure's velocity response is measured by a continuously SLVD (CSLDV) system including spatial- and time-domain information. Since the structure's velocity is recorded during the test, a different signal processing approach is required to determine the deflection shape and dynamic characteristics of the structure [31]. Two CSLDV measurement approaches have been developed by Stanbridge and Ewins [32] to determine the operating deflection shapes of a system subjected to sinusoidal excitation. Allen and Sracic [33] suggested a lifting approach to determine the modal characteristics of the structures using conventional curve-fitting methods. These approaches were applied with various scan trajectories, including area scans, line scans, and circular scans.

Experimental investigations on the dynamic characteristics of modular structures are limited to the works conducted by Alembagheri et al. [34], Rashidi et al. [35], and Sharafi et al. [36]. Alembagheri et al. studied the contribution of different configurations and arrangements of infill walls on the natural frequencies of a modular unit. They showed that adding infill walls can decrease the frequencies of the modular unit by up to 50% [34]. Rashidi et al. [35] conducted experimental tests and numerical simulations to investigate the effect of gypsum and cement-board light-steel-framed composite walls on the natural frequencies and damping ratios of a modular unit. Sharafi et al. [36] performed an experimental and numerical study on the system identification of modular steel frames in a laboratory environment. They employed different techniques of operational modal analysis to determine the modal properties of modular frames.

In this experimental study, which is a part of a broad project on compliance criteria for the design of inter-connections in modular buildings in progress at Western Sydney University (WSU), the dynamic characteristics of a modular structure, including natural frequencies, mode shapes, and damping ratios, were identified. To that end, a half-scaled three-storey modular structure was fabricated in a factory, transported, and fixed to the structural lab of the Centre for Infrastructure Engineering (CIE) at WSU. The modular structure was instrumented with highly sensitive accelerometers at different locations

to record its acceleration response under pure and randomly generated vibration due to hammer impacts. The recorded acceleration response of the structure was analysed using different techniques to extract the natural frequencies and their corresponding mode shapes and damping ratios.

2. Modal Test Methods

The fundamental objective of system identification of a structure is to extract its dynamic characteristics, including natural frequencies, mode shapes, and damping ratios. Among them, natural frequencies and mode shapes can be determined from numerical simulations. However, there are some uncertainties in numerical simulations that affect the natural dynamic characteristics. These uncertainties include stiffness uncertainties of connections and material uncertainties, indicating the need to conduct experimental analysis. Moreover, the most reliable approach to evaluate the damping ratios of a system is conducting experimental tests on the structure under realistic conditions. The damping ratio of a system is an important parameter that plays a crucial role in the performance of a structure against earthquake and wind actions. The higher the damping ratio, the less the response of a system under lateral loads. Extensive research has been conducted on the system identification of high-rise structures, cable-stayed bridges, dams, and liquid storage tanks [37–41]. System identification methods are classified into two groups: experimental modal analysis (EMA) and operational modal analysis (OMA) [42]. In EMA, the dynamic characteristics of a system are identified through the signal processing of the response acceleration of the system to several known forces. Therefore, to determine the modal properties of a system, both input force and output response should be measured. On the other hand, in OMA, the dynamic characteristics of a structure can be determined through the signal processing of the response acceleration of the system to several arbitrary generated forces. Because OMA is non-destructive, economical, and fast to implement and does not require special equipment, it is preferred over EMA. According to OMA, several techniques can be used to calculate the dynamic characteristics of a system. These techniques are the peak-picking method (PP), enhanced frequency-domain decomposition (EFDD), and stochastic subspace identification (SSI), which are described as follows.

2.1. Peak-Picking (PP) Method

One of the simplest yet accurate methods to extract the natural frequencies of a system is the peak-picking (PP) method. In this method, recorded responses of a system, mainly acceleration, are transformed to the frequency domain using the fast Fourier transform. Then, the peak values of the frequency of the auto-spectra are chosen to determine the frequencies corresponding to the resonant frequencies of the system.

2.2. Enhanced Frequency-Domain Decomposition (EFDD)

This method is based on the frequency domain. According to the EFDD technique, the relation between an unknown input force $f(t)$ and the recorded response of structure $u(t)$ is represented as [43]:

$$[G_{uu}(j\omega)] = [H(j\omega)]^* [G_{ff}(j\omega)] [H(j\omega)]^T \quad (1)$$

where $G_{uu}(j\omega)$ is the power spectral density (PSD) matrix of the response of the structure, $G_{ff}(j\omega)$ is the PSD matrix of the input force f , $H(j\omega)$ is the frequency response function, and * and T are the complex conjugate and transpose, respectively. The equation can be solved by conducting singular value decomposition (SVD) of the determined PSD matrices. The results of the equation obtained from decomposition illustrate that the singular values are estimates of the auto-spectra of the system or natural frequencies, and singular values are estimates of mode shapes [44]. The theory of the EFDD method is described in detail in [45].

2.3. Stochastic Subspace Identification (SSI)

This method is based on the time domain, in which a parametric model is fitted directly to the time series of the recorded responses of a structure. The fitted parametric model is a mathematical model with some adjustable variation and parameters that can be changed to fit the mathematical model to the recorded data. In general, it is required to determine a set of parameters to minimise the deviation between the measured response of the structure and the predicted system response of the model. In this method, the state-space formulation of the system is decomposed into frequencies and modes, while the damping of the structure is evaluated from the complex frequency [44]. The theory of the SSI method is described in detail in [46]. The ARTeMIS extractor software [47] was employed in this study to determine the natural frequencies, damping ratios, and mode shapes.

3. Description of Testing and Instrumentation

Figure 2a depicts the 3D view of the test specimen. Modules were fabricated in a factory, transported to the structural laboratory of CIE at WSU, and fixed to the strong floor. Each column is connected to the strong floor by four M12 bolts. The lateral-load-resisting system of the structure against wind and earthquake actions is provided by moment-resisting frames. The designed modular building has one bay in both longitudinal and transverse directions. Each module has a length, width, and height of 2.4, 1.2, and 1.5 m, respectively. The test specimen comprises three half-scaled modular units that are connected vertically, so the total height of the building is 4.5 m. The structure was designed based on the Australian standard for the design of steel structures (AS 4100) [48] and the Australian standard for the design of structures against wind actions (AS1170.2) [49]. The details of each modular unit in both longitudinal and transverse directions are shown in Figure 2b,c, respectively.

Beams at floor and ceiling levels are made of PFC100 in both longitudinal and transverse directions. Columns are made of SHS100 × 100 × 4 mm, which is a typical section for columns in modular structures. Joists are made of light steel sections C10015, in which they are connected to longitudinal beams at both ceiling and floor levels. The distance between joists is considered to be 400 mm, and the distance between the first joists to the column is considered to be 300 mm. Joists are connected to the web of beams by employing angles having 50 × 50 × 5 mm sections, which are bolted to joists by two M8 bolts and welded to the web of beams by fillet weld, as shown in Figure 2d. The connectivity of modules is provided by vertical inter-connections at the corners of each module. The details of bolted end-plate connections employed to connect the modules together are illustrated in Figure 2e. The bolted end-plate connection comprises an end plate, which is welded to the ends of columns using fillet weld and four M10 high-strength grade 8.8 bolts. The hole diameters are 12 mm, 2 mm wider than bolt diameters, to take into account practical constraints in manufacturing and assembly. The bolted connection was chosen as the intra-connection to provide connectivity between beams and columns. Figure 2f illustrates the details of intra-connections used in this experimental test. The connection includes two 200 mm × 70 mm × 6 mm plates, which are welded to the column and connected to the beam through two shim plates and eight M12 high-strength grade 8.8 bolts. While moment action in beams is transferred from beams to columns through the combination of plates and bolts, shear action is transferred by the use of shear tabs, which are welded to columns. The connectivity between shear tabs and beams is provided by welding shear tabs to beams. The mass of each floor corresponding to dead and live loads is considered to be 300 kg. Artificial masses were placed on the second and third floors of the test specimen, as well as the ceiling at the third level. Figure 3 shows the artificial mass used to apply dead and live loads.

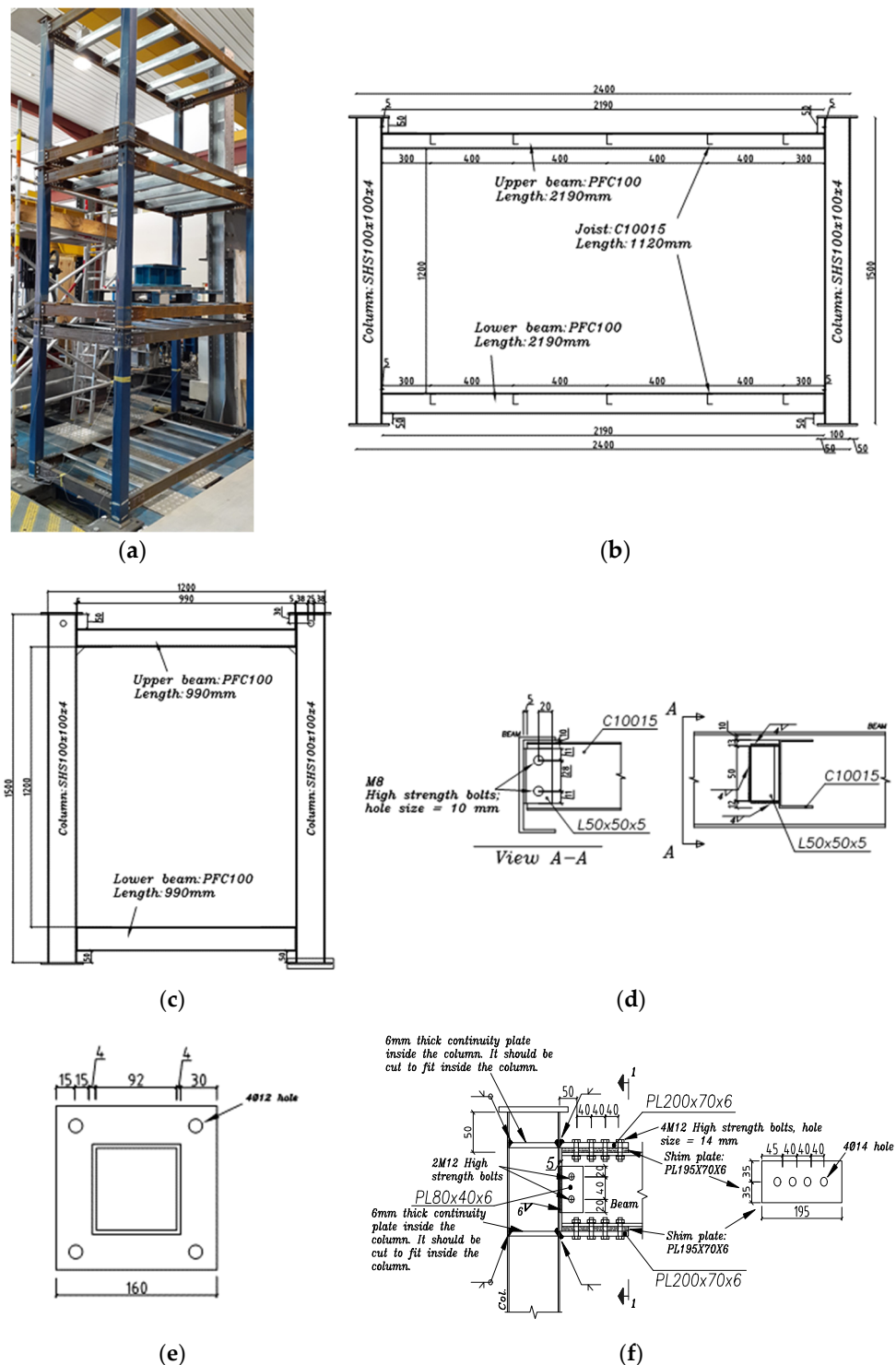


Figure 2. (a) Three-dimensional view of the test specimen; (b) details of a modular unit in the longitudinal direction; (c) details of a modular unit in the transverse direction; (d) details of joist connections; (e) details of inter-connections; (f) details of intra-connections.

The determination of dynamic characteristics of a system, based on the OMA method, needs to monitor and record responses of the system under different types of vibration, including free and ambient vibrations. In this method, the time history of the input forces is not required to be recorded. Therefore, to record the responses of the structure, it is instrumented with five highly sensitive accelerometers. The accelerometers are single-axis accelerometers, which are connected to the tops of columns by heated glue at ceiling levels

of different storeys along the middle axis of columns. Figure 4 shows an accelerometer attached to the column of the test specimen. A data acquisition system is employed to monitor and record the time history of responses. The accelerometers are micro-electro-mechanical systems (MEMS) produced by Silicon Design Accelerometers and connected to the data acquisition system with shielded four-core cables having low noise. In order to monitor and record the responses of the structure, the LabVIEW software, which supports the data acquisition system, is employed. The software can record 1000 samples per second, corresponding to the nominal Nyquist frequency of 500 Hz.



Figure 3. Artificial mass, placed on the test specimen.

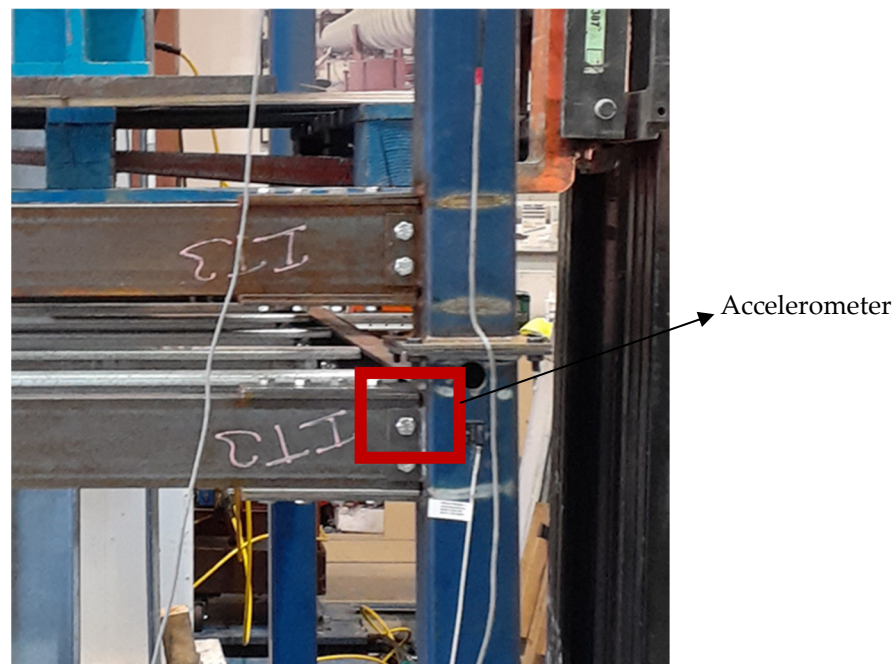


Figure 4. An accelerometer attached to the column of the specimen.

A step-by-step experimental program was conducted to determine the natural dynamic characteristics of the structure. In the first step (test case 1), the acceleration response of the structure was recorded under pure vibration without imposing any external excitation. On the other hand, in steps 2 through 10 (test cases 2 to 10), the acceleration responses of the structure were recorded under randomly generated vibration by hammer impacts at different locations, depicted in Figure 5. These locations are the tops of columns at the first storey, the middle of columns at the second storey, and the middle of the joist at the

ceiling level of the first storey. Accelerometers are named based on their orientation, as shown in Figure 5. Accelerometers oriented along the transverse direction of the structure are named 2L and 3L, and accelerometers oriented along the longitudinal direction of the structure are named 1S to 3S. Because of the low amplitude of excitation that may occur in the structure, highly sensitive accelerometers with a sensitivity of 2 V/g were used to record the acceleration response of the system. The technical properties of accelerometers used in this experimental test are tabulated in Table 1.

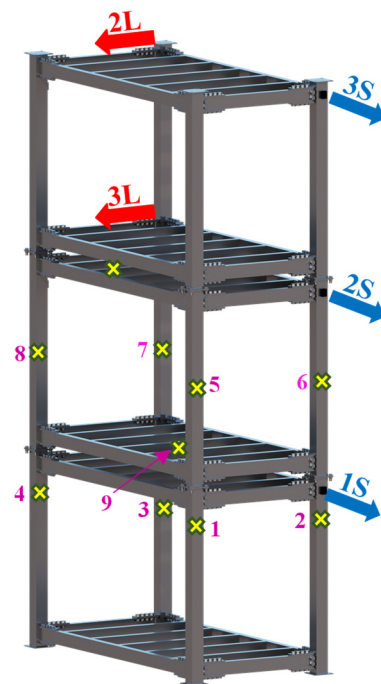


Figure 5. Location of hammer impacts, sensor names, and orientation.

Table 1. Specifications of accelerometers used in this experimental test.

Operational Properties	Value
Output voltage	± 16 V
Full-scale range	2 g
Cross-axis sensitivity	$\pm 2\%$
Nonlinearity	$\pm 0.15\%$
Bias calibration error	± 30 mV
Output noise (RMS, typical)	$10 \mu\text{g}/(\text{root Hz})$
Operating temperature	-55 to $+125$ °C

4. Results and Discussion

This section provides information about the natural frequencies, mode shapes, and damping ratios extracted through different signal processing techniques of the recorded acceleration response of the test specimen.

4.1. Peak-Picking Method

Figure 6 shows the time histories of the acceleration response of the test specimen recorded by accelerometer 3L for different test cases. The figure illustrates that different levels of acceleration, occurring at different times, were generated in the test specimen due to hammer impacts. Generating different intensities of acceleration is required to make sure that all modes of the structure are excited.

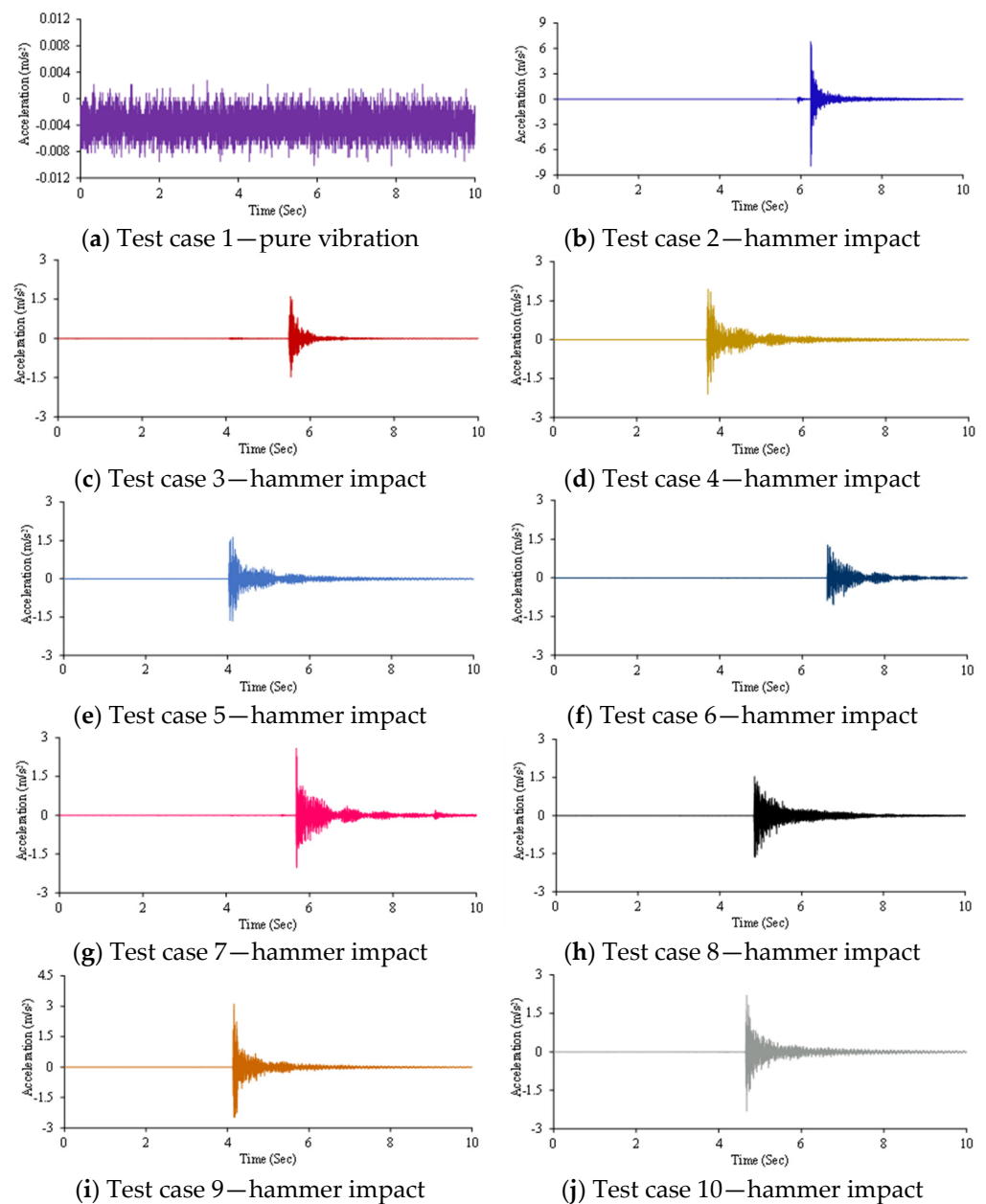


Figure 6. Time histories of response acceleration of test specimen recorded by accelerometer 3L in different test cases.

The fast Fourier transform (FFT) of recorded accelerations for different test cases is presented in Figure 7. The figures indicate an increase in the signal-to-noise ratio in test cases 2 to 10 compared to that of test case 1, in which the structure was tested under pure vibration. With reference to Figure 7a, no clear peaks can be observed in the FFT of the response acceleration of the test specimen. Therefore, the natural frequencies of the structure cannot be identified from the pure vibration test, in which no external force is imposed on the structure. However, the FFT of responses obtained from sensors 3L and 2L have a higher amplitude in the range of 4–6 Hz compared to those obtained from other sensors. Moreover, the figure shows that the FFT amplitude of the acceleration response recorded by sensor 2S has a higher value compared to those of other sensors near a frequency of 50 Hz. This indicates that one of the structure's natural frequencies lies in the range of 4–6 Hz, and the other one is around 50 Hz. The former corresponds to the transverse direction, and the latter corresponds to the longitudinal direction.

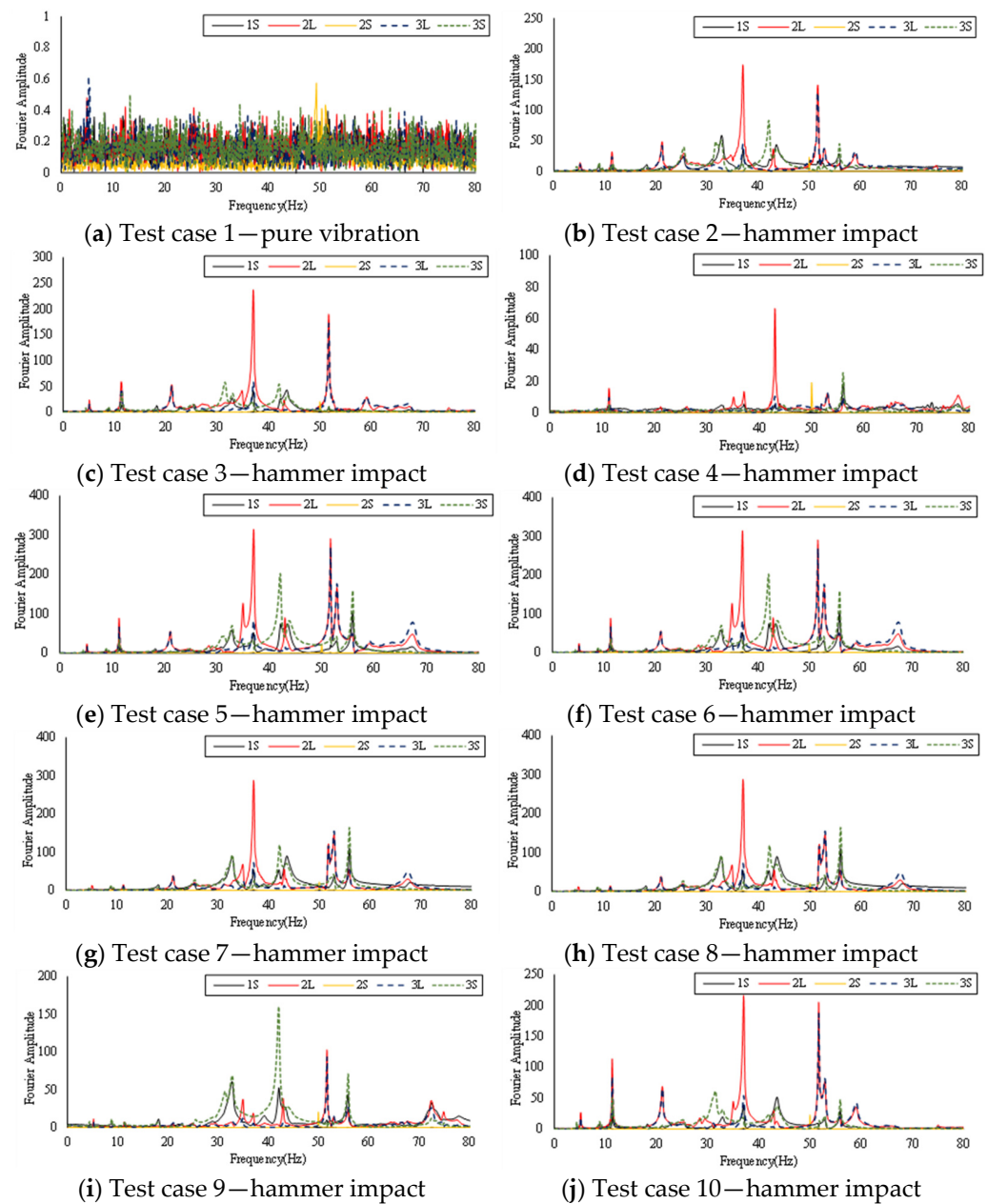


Figure 7. Fast Fourier transforms of recorded accelerations.

Figure 7b–j shows the FFT of the recorded acceleration of the structure in the hammer impact test. It is seen that the amplitude, direction, and location of hammer impacts influence the excited modes of the test specimen. Imposing a randomly generated vibration on the structure significantly excites the modes of the test specimen. According to Figure 7b–j, the first peak is observed around 4.9 Hz for all test cases, except test case 4, which was recorded by sensor 3S. Therefore, this mode is probably related to the longitudinal direction. The second mode recorded by sensors 2L and 3L occurs around 5.3 Hz, which is related to the transverse direction. The FFT of the response acceleration shows a peak at 8.7 Hz, which is observed at both 3L and 3S sensors. This indicates that the mode is probably related to the torsional direction. Moving to higher modes, two peaks are observed in the range of 10–20 Hz. The first peak in this range is observed at 11.23 Hz, corresponding to the longitudinal direction. This mode is observed in all test cases. On the other hand, the second peak in the range of 10–20 Hz occurs at 18.06 Hz, related to the transverse direction. The fifth peak in the FFT of responses can be observed around a frequency of 21 Hz, corresponding to the longitudinal direction. This mode was recorded by sensors 2L

and 3L in different test cases except for test cases 3 and 8. The next natural frequency of the structure is observed at 25.39 Hz, which is related to the transverse direction. In the range of 30–40 Hz, two distinct modes can be observed in all test cases. The first mode in this range occurs at a frequency of 31.2 Hz, and the second mode of the structure is observed at a frequency of 36.9 Hz. The former corresponds to the longitudinal direction, and the latter relates to the torsional direction. Some other peaks are observed at 40–70 Hz. However, for frequencies higher than 70 Hz, no distinct modes can be observed.

Based on the obtained responses, the FFT of responses was averaged for individual sensors for different test cases. A summary of the FFT diagrams and the clear peaks are depicted in Figure 8. The identified natural frequencies of the structure are validated using EFDD and SSI methods in the next sections.

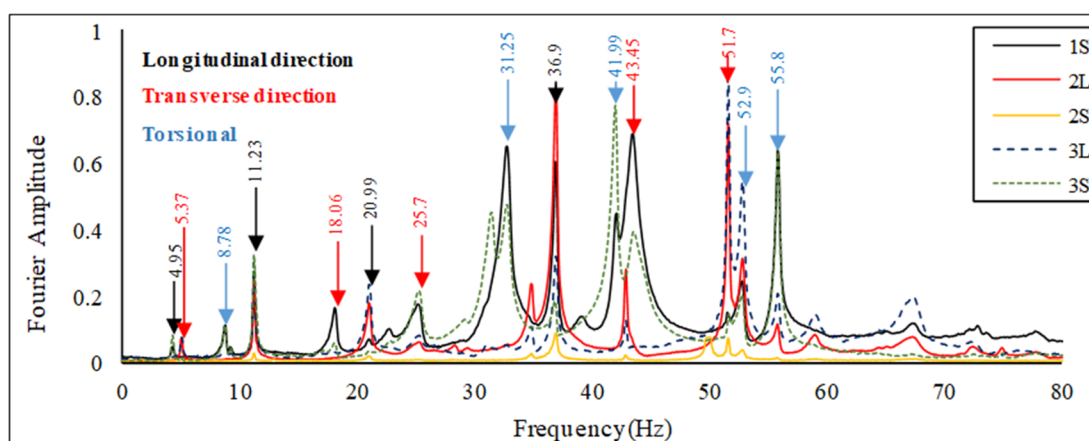


Figure 8. FFT of responses for various sensors averaged over the different cases.

4.2. EFDD Method

The EFDD method uses the SVD of the power spectral density of the acceleration response of the structure to analyse data in the frequency domain. The EFDD method was employed to validate the modes extracted by the FFT method in the previous section. The SVD of the acceleration response of the structure corresponding to different test cases, along with some identified frequencies, is shown in Figure 9.

According to the SVD of the acceleration response obtained from pure vibration, two clear peaks are observed. The first peak lies in the range of 4–6 Hz, and the second peak occurs around 50 Hz. These frequencies are the same as those obtained with the FFT method. For other test cases, the peaks corresponding to the different natural frequencies of the test specimen were identified and picked. Through the investigation of SVD of responses of the test specimen, the peaks associated with various natural frequencies can be chosen so that they can be extracted from different test cases. The first six extracted natural frequencies and damping ratios of the test specimen are tabulated in Tables 2 and 3, respectively. The results indicate that almost all modes can be identified in all test cases, except the first test case, which is pure vibration. However, some modes of the test specimen cannot be identified in some test cases. For example, the fifth frequency (18.06 Hz) is not observed in test case 7. The signal processing of the acceleration response data illustrates that the damping ratio corresponding to the first natural frequency is 5.4%, and it is 5.2% for the second mode of the structure.

In addition to the natural frequencies and damping ratios, the mode shapes corresponding to each natural frequency are presented in Figure 10 for the first five modes of the test specimen. The figure suggests that the first mode of the structure has a translational shape along the longitudinal direction. The second mode of the structure, which is a translational mode, occurs along the transverse direction. These modes are fundamental modes of the structure along the longitudinal and transverse directions. The third and fourth modes of the structure are torsional and longitudinal modes.

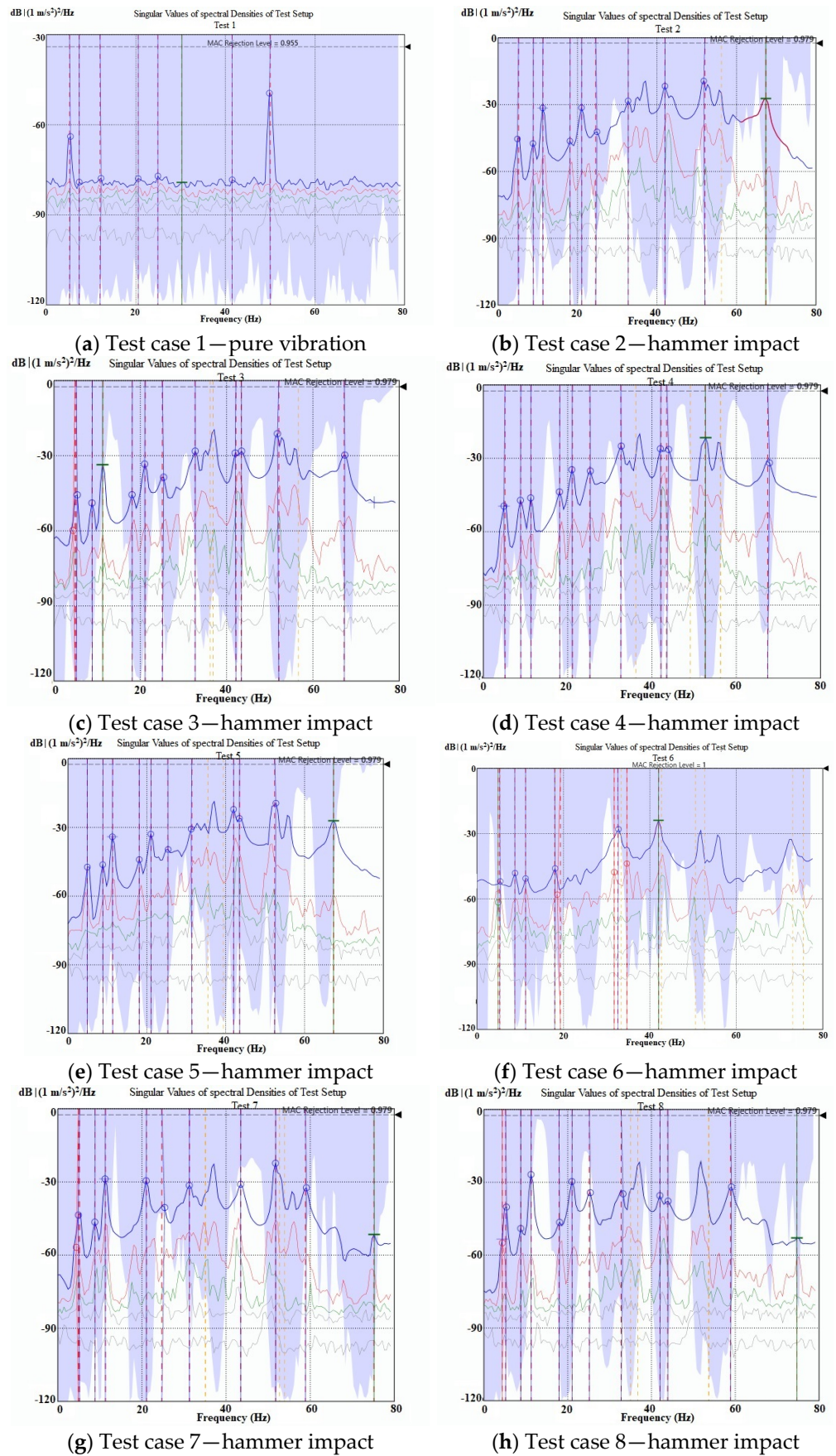


Figure 9. Cont.

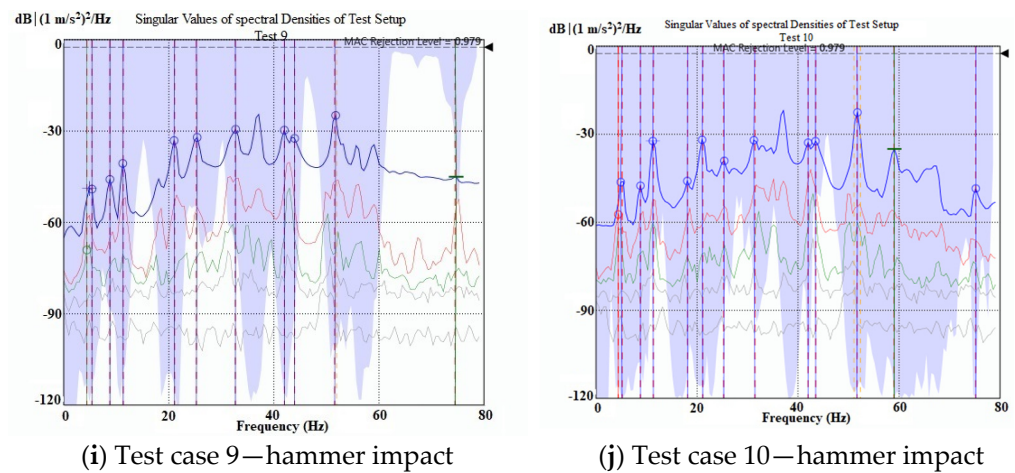


Figure 9. SVD of the acceleration response, along with identified frequencies.

Table 2. Extracted natural frequencies using the EFDD method.

Mode No.	Test Case									
	Test1 (Hz)	Test2 (Hz)	Test3 (Hz)	Test4 (Hz)	Test5 (Hz)	Test6 (Hz)	Test7 (Hz)	Test8 (Hz)	Test9 (Hz)	Test10 (Hz)
1	4.9	4.43	4.32	4.35	4.81	4.79	4.962	4.83	4.82	4.32
2	5.46	5.19	5.213	5.06	5.10	5.11	5.236	5.05	5.15	5.18
3	8.43	8.84	8.51	8.79	8.71	8.536	8.92	8.71	8.751	8.86
4	11.2	11.25	11.38	11.02	11.46	11.13	11.21	11.876	11.44	11.342
5	18.41	18.51	18.3	18.103	18.02	18.05	-	17.98	18.34	18.12

Table 3. Extracted damping ratios using the EFDD method.

Mode No.	Test Case									
	Test1 (%)	Test2 (%)	Test3 (%)	Test4 (%)	Test5 (%)	Test6 (%)	Test7 (%)	Test8 (%)	Test9 (%)	Test10 (%)
1	5.31	5.41	5.35	5.42	5.39	5.43	5.36	5.38	5.40	5.17
2	5.12	5.15	5.25	5.28	5.11	5.17	5.23	5.2	5.16	5.22
3	4.12	4.09	4.1	4.11	4.13	4.08	4.07	4.15	4.07	4.14
4	2.81	2.79	2.76	2.83	2.82	2.75	2.7	2.89	2.71	2.73
5	2.12	2.14	2.1	2.09	2.11	2.15	-	2.13	2.05	2.07

4.3. SSI Method

The SSI technique, which is based on the time domain, was used to identify the natural characteristics of the test specimen through the signal processing of the same recorded acceleration response. Figure 11a,b illustrate the stabilisation diagrams of state-space models of test cases 6 and 10, respectively. The eigenvectors and eigenvalues of the dynamic matrix of the model, which are indicative of the natural frequencies and mode shapes of the structure, can be determined from the stabilisation diagrams. The determined natural frequencies and mode shapes are independent of the order of the numerical model and process. The natural frequencies and damping ratios of the test specimen extracted using the SSI technique are listed in Tables 4 and 5, respectively.

The natural frequencies listed in Table 5 show that they are almost identical to those obtained through the EFDD technique, indicating that the obtained results are reliable. The investigation shows that no natural frequency can be identified for test cases 7, 9, and 1, in which the modular structure was examined under pure vibration, which is not depicted here. The results indicate that the sequence of natural frequencies obtained from

the SSI technique is the same as that obtained with the EFDD technique, in which the first, second, and third modes are related to the longitudinal, transverse, and torsional directions. The investigation of higher modes illustrates that the fourth and fifth modes are related to the longitudinal and transverse directions. The damping ratios corresponding to each test case and natural frequency, listed in Table 5, demonstrate that while in some test cases, there is a good agreement between the results of the EFDD and SSI techniques, in other cases, the difference in the obtained damping ratios through the EFDD and SSI techniques reaches more than 15%. Hence, the SSI technique is unable to forecast the damping ratios consistently.

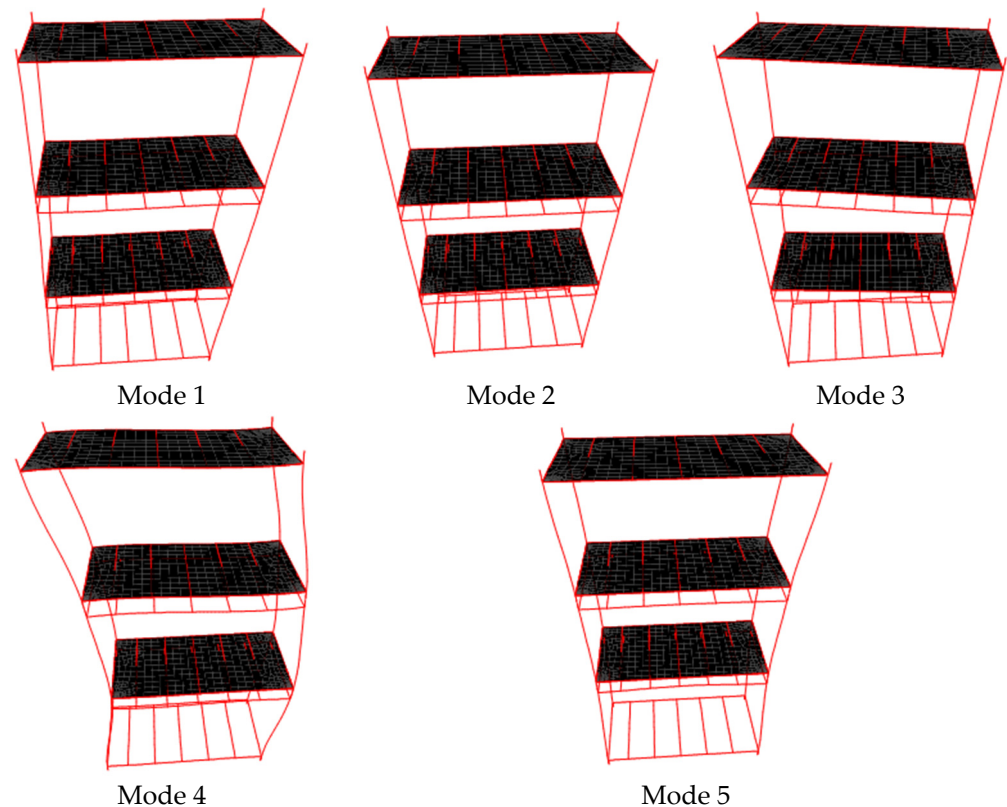


Figure 10. Identified mode shapes of the test specimen.

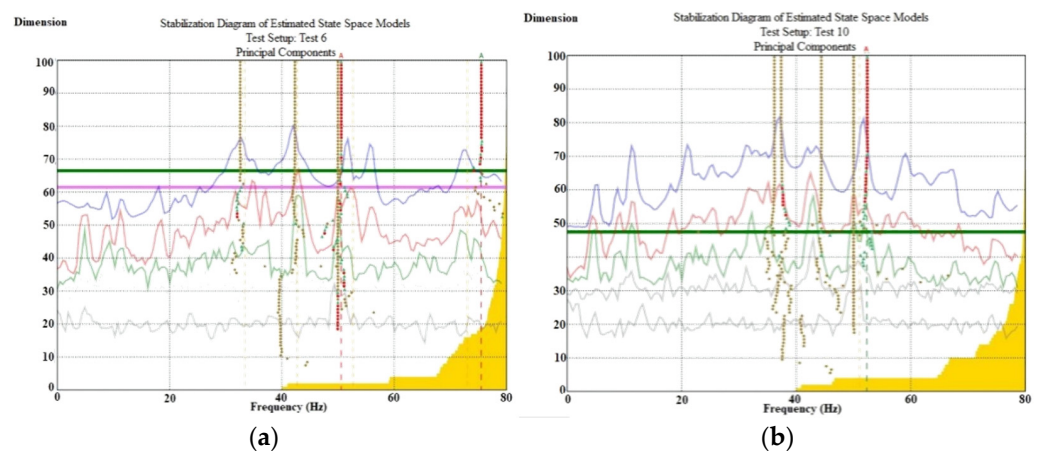


Figure 11. Stabilisation diagram of estimated state-space models of (a) test case 6—hammer impact; (b) test case 10—hammer impact.

Table 4. Extracted natural frequencies using the SSI method.

Test Case										
Mode No.	Test1 (Hz)	Test2 (Hz)	Test3 (Hz)	Test4 (Hz)	Test5 (Hz)	Test6 (Hz)	Test7 (Hz)	Test8 (Hz)	Test9 (Hz)	Test10 (Hz)
1	-	4.24	-	4.26	5.124	-	-	-	-	-
2	-	-	5.51	-	-	-	5.2	-	5.21	-
3	-	8.95	-	8.97	-	-	8.91	8.49	8.85	-
4	-	-	-	-	-	11.27	11.53	11.61	-	-
5	18.301	18.5	-	18.73	18.61	-	-	-	18.29	18.41

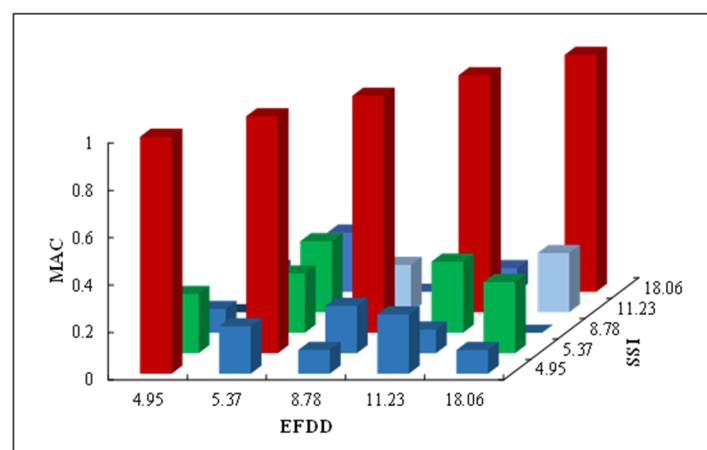
Table 5. Extracted damping ratios using the SSI method.

Test Case										
Mode No.	Test1 (%)	Test2 (%)	Test3 (%)	Test4 (%)	Test5 (%)	Test6 (%)	Test7 (%)	Test8 (%)	Test9 (%)	Test10 (%)
1	-	5.21	-	5.65	5.54	-	-	-	-	-
2	-	-	5.28	-	5.21	-	-	5.13	-	-
3	-	2.41	2.4	2.16	-	-	-	2.58	-	-
4	-	-	-	1.55	-	1.43	-	1.2	-	-
5	-	1.05	-	1.23	0.91	-	-	-	-	1.07

The correlation between two mode shapes extracted through two techniques can be evaluated using the modal assurance criterion (MAC). In this paper, the MAC value is used to compare the mode shapes obtained with the EFDD method with the ones extracted using the SSI method. The MAC value is expressed as [50]:

$$MAC_{EFDD,SSI} = \frac{(\varphi_{EFDD,A}^T \varphi_{SSI,B})^2}{(\varphi_{EFDD,A}^T \varphi_{EFDD,A})(\varphi_{SSI,B}^T \varphi_{SSI,B})} \quad (2)$$

where $\varphi_{EFDD,A}$ and $\varphi_{SSI,B}$ are mode shapes A and B of the structure extracted by the EFDD and SSI algorithms, respectively. The MAC can be in the range of 0 to 1, where a value of unity indicates a perfect correlation between the two identified modes, and a value of zero illustrates that the two identified modes are orthogonal and have no similarity. Figure 12 shows the MAC values of the first five identified modes of the structure. The results indicate that the correlation between the extracted modes lies between 0.95 to 1, illustrating a perfect correlation between the identified modes in frequency and time domains. The results show that both methods can be efficiently employed as an output-only algorithm.

**Figure 12.** The MAC values between extracted modes through SSI and EFDD techniques.

5. Conclusions

In this experimental work, the modal properties of a half-scaled three-storey modular structure were identified under free and ambient vibrations. The test specimen was fixed to a strong floor and instrumented with highly sensitive accelerometers at different locations. The acceleration responses of the structure were recorded under pure vibration and ambient vibration in different test cases. The randomly generated force for the ambient vibration was produced by a hammer impact. The main dynamic characteristics of the modular structure, including natural frequencies, damping ratios, and mode shapes, were extracted by employing different techniques of operational modal analysis (OMA). These techniques are FFT peak picking (PP), enhanced frequency-domain decomposition (EFDD), and stochastic subspace identification (SSI). The conclusions of this study can be drawn as follows:

- Compared to pure vibration, the signal-to-noise ratio increased when inducing external excitation due to hammer impacts; therefore, the natural dynamic characteristics cannot be extracted from pure vibration.
- The direction, amplitude, and placement of the hammer impact significantly influenced the excited modes. Therefore, various tests should be conducted to completely identify the frequencies of the structure.
- Good agreement was observed between the results of the PP and EFDD methods.
- The SSI method, which is based on the time domain, could not identify all modes in different test cases. Hence, this method can be employed to control the frequencies obtained by the EFDD method.
- A damping ratio of 5.4% corresponding to the first mode of the structure was determined through the use of the EFDD method.
- When moving to higher modes, the damping ratio of the structure decreased.
- The first frequency of the structure was observed at 4.95 Hz, and the second one was observed at 5.37 Hz, showing that the structure's frequency increases when moving to higher modes.

Author Contributions: Conceptualization, M.F.; methodology, M.F., P.S., A.B. and H.E.; software, A.B. and H.E.; validation, A.B.; formal analysis, M.F., A.B. and H.E.; investigation, M.F.; resources, P.S. and P.R.; data curation, A.B.; writing—original draft preparation, M.F. and H.E.; writing—review and editing, P.S. and P.R.; visualization, A.B.; supervision, P.S. and P.R.; project administration, P.S.; funding acquisition, P.S. and P.R. All authors have read and agreed to the published version of the manuscript.

Funding: This research was funded by Australian Research Council (ARC) grant number DE190100113 and The APC was funded by Western Sydney University.

Institutional Review Board Statement: Not applicable.

Informed Consent Statement: Not applicable.

Data Availability Statement: Not applicable.

Acknowledgments: The authors acknowledge the support of Australian Research Council (ARC) grant DE190100113 for this research project and the writing of this paper.

Conflicts of Interest: The authors declare no potential conflicts of interest with respect to the research, authorship, and/or publication of this article.

References

1. Srisangeerthan, S.; Hashemi, M.J.; Rajeev, P.; Gad, E.; Fernando, S. Numerical study on the effects of diaphragm stiffness and strength on the seismic response of multi-story modular buildings. *Eng. Struct.* **2018**, *163*, 25–37. [\[CrossRef\]](#)
2. Lawson, M.; Ogden, R.; Goodier, C.I. *Design in Modular Construction*; CRC Press: Boca Raton, FL, USA, 2014.
3. Lawson, R.M.; Grubb, P.J.; Prewer, J.; Trebilcock, P.J. *Modular Construction Using Light Steel Framing: An Architect's Guide*; Steel Construction Institute: Berkshire, UK, 1999.

4. Farajian, M.; Sharafi, P.; Kildashti, K. The influence of inter-module connections on the effective length of columns in multistory modular steel frames. *J. Constr. Steel Res.* **2021**, *177*, 106450. [[CrossRef](#)]
5. WilliamLacey, A.; Chen, W.; Hao, H.; Bi, K. Effect of inter-module connection stiffness on structural response of a modular steel building subjected to wind and earthquake load. *Eng. Struct.* **2020**, *213*, 110628.
6. Sharafi, P.; Hadi, M.N.; Teh, L.H. Optimum Column Layout Design of Reinforced Concrete Frames Under Wind Loading. In *Topics on the Dynamics of Civil Structures*; Springer: New York, NY, USA, 2012; Volume 1, pp. 327–340.
7. Sharafi, P.; Hadi, M.N.; Teh, L.H. Optimum Spans' Lengths of Multi-Span reinforced Concrete Beams Under Dynamic Loading. In *Topics on the Dynamics of Civil Structures*; Springer: New York, NY, USA, 2012; Volume 1, pp. 353–361.
8. Kaveh, A.; Sharafi, P. Ant colony optimization for finding medians of weighted graphs. *Eng. Comput.* **2008**, *25*, 102–120. [[CrossRef](#)]
9. Kaveh, A.; Sharafi, P. Nodal ordering for bandwidth reduction using ant system algorithm. *Eng. Comput.* **2009**, *26*, 313–323. [[CrossRef](#)]
10. Kaveh, A. Ordering for bandwidth and profile minimization problems via charged system search algorithm. *Iran. J. Sci. Technol. Trans. B Eng.* **2012**, *36*, 39–52.
11. Chen, Z.; Liu, J.; Yu, Y.; Zhou, C.; Yan, R. Experimental study of an innovative modular steel building connection. *J. Constr. Steel Res.* **2017**, *139*, 69–82. [[CrossRef](#)]
12. Chen, Z.; Liu, J.; Yu, Y. Experimental study on interior connections in modular steel buildings. *Eng. Struct.* **2017**, *147*, 625–638. [[CrossRef](#)]
13. Sanches, R.; Mercan, O.; Roberts, B. Experimental investigations of vertical post-tensioned connection for modular steel structures. *Eng. Struct.* **2018**, *175*, 776–789. [[CrossRef](#)]
14. Lee, S.; Park, J.; Shon, S.; Kang, C. Seismic performance evaluation of the ceiling-bracket-type modular joint with various bracket parameters. *J. Constr. Steel Res.* **2018**, *150*, 298–325. [[CrossRef](#)]
15. Gunawardena, T.; Ngo, T.; Mendis, P. Behaviour of multi-storey prefabricated modular buildings under seismic loads. *Earthq. Struct.* **2016**, *11*, 1061–1076. [[CrossRef](#)]
16. Fathieh, A.; Mercan, O. Seismic evaluation of modular steel buildings. *Eng. Struct.* **2016**, *122*, 83–92. [[CrossRef](#)]
17. Landolfo, R.; Iuorio, O.; Fiorino, L. Experimental seismic performance evaluation of modular lightweight steel buildings within the ELISSA project. *Earthq. Eng. Struct. Dyn.* **2018**, *47*, 2921–2943. [[CrossRef](#)]
18. Sendanayake, S.V.; Thambiratnam, D.P.; Perera, N.; Chan, T.; Aghdamy, S. Seismic mitigation of steel modular building structures through innovative inter-modular connections. *Heliyon* **2019**, *5*, e02751. [[CrossRef](#)] [[PubMed](#)]
19. Feng, R.; Shen, L.; Yun, Q. Seismic performance of multi-story modular box buildings. *J. Constr. Steel Res.* **2020**, *168*, 106002. [[CrossRef](#)]
20. Sendanayake, S.V.; Thambiratnam, D.P.; Perera, N.J.; Chan, T.H.T.; Aghdamy, S. Enhancing the lateral performance of modular buildings through innovative inter-modular connections. *Structures* **2021**, *29*, 167–184. [[CrossRef](#)]
21. Bagheri, S.; Farajian, M. The effects of input earthquake characteristics on the nonlinear dynamic behavior of FPS isolated liquid storage tanks. *J. Vib. Control* **2018**, *24*, 1264–1282. [[CrossRef](#)]
22. Farajian, M.; Khodakarami, M.I.; Kontoni, D.P.N. Evaluation of Soil-Structure Interaction on the Seismic Response of Liquid Storage Tanks under Earthquake Ground Motions. *Computation* **2017**, *5*, 17. [[CrossRef](#)]
23. Karkabadi, A.; Khodakarami, M.I.; Farajian, M. Seismic Response of Steel Frame by Considering Soil-Structure Interaction under Seismic Sequence. *J. Struct. Constr. Eng.* **2021**, *8*, 66–86.
24. Farajian, M.; Khodakarami, M.I.; Sharafi, P. Effect of MetaFoundation on the Seismic Responses of Liquid Storage Tanks. *Appl. Sci.* **2022**, *12*, 2514. [[CrossRef](#)]
25. Kawashima, S.; Fujimoto, T. Vibration analysis of frames with semi-rigid connections. *Comput. Struct.* **1984**, *19*, 85–92. [[CrossRef](#)]
26. Goksu, C.; Inci, P.; Demir, U.; Yazgan, U.; Ilki, A. Field testing of substandard RC buildings through forced vibration tests. *Bull. Earthq. Eng.* **2017**, *15*, 3245–3263. [[CrossRef](#)]
27. Memari, A.M.; Aghakouchak, A.A.; Ashtiani, M.G.; Tiv, M. Full-scale dynamic testing of a steel frame building during construction. *Eng. Struct.* **1999**, *21*, 1115–1127. [[CrossRef](#)]
28. Sophianopoulos, D. The effect of joint flexibility on the free elastic vibration characteristics of steel plane frames. *J. Constr. Steel Res.* **2003**, *59*, 995–1008. [[CrossRef](#)]
29. Türker, T.; Bayraktar, A. Finite element model calibration of steel frame buildings with and without brace. *J. Constr. Steel Res.* **2013**, *90*, 164–173. [[CrossRef](#)]
30. Rothberg, S.J.; Allen, M.S.; Castellini, P.; Di Maio, D.; Dirckx, J.J.J.; Ewins, D.J.; Halkona, B.J.; Muyschondt, P.; Paonec, N.; Ryan, T.; et al. An international review of laser Doppler vibrometry: Making light work of vibration measurement. *Opt. Lasers Eng.* **2017**, *99*, 11–22. [[CrossRef](#)]
31. Sriram, P.; Hanagud, S.; Craig, J. *Mode Shape Measurement Using a Scanning Laser Doppler Vibrometer*. "Vol. 1 Florence."; Union Coll: Schenectady, NY, USA, 1991; pp. 176–181.
32. Stanbridge, A.; Ewins, D. Modal testing using a scanning laser Doppler vibrometer. *Mech. Syst. Signal Process.* **1999**, *13*, 255–270. [[CrossRef](#)]
33. Allen, M.S.; Sracic, M.W. A new method for processing impact excited continuous-scan laser Doppler vibrometer measurements. *Mech. Syst. Signal Process.* **2010**, *24*, 721–735. [[CrossRef](#)]
34. Alembagheri, M.; Sharafi, P.; Rashidi, M.; Bigdeli, A.; Farajian, M. Natural dynamic characteristics of volumetric steel modules with gypsum sheathed LSF walls: Experimental study. *Structures* **2021**, *33*, 272–282. [[CrossRef](#)]
35. Rashidi, M.; Sharafi, P.; Alembagheri, M.; Bigdeli, A.; Samali, B. Operational modal analysis, testing and modelling of prefabricated steel modules with different LSF composite walls. *Materials* **2020**, *13*, 5816. [[CrossRef](#)]

36. Sharafi, P.; Rashidi, M.; Alembagheri, M.; Bigdeli, A. System Identification of a Volumetric Steel Modular Frame Using Experimental and Numerical Vibration Analysis. *J. Archit. Eng.* **2021**, *27*, 04021032. [[CrossRef](#)]
37. Brownjohn, J.M. Ambient vibration studies for system identification of tall buildings. *Earthq. Eng. Struct. Dyn.* **2003**, *32*, 71–95. [[CrossRef](#)]
38. Wilson, J.C.; Liu, T. Ambient vibration measurements on a cable-stayed bridge. *Earthq. Eng. Struct. Dyn.* **1991**, *20*, 723–747. [[CrossRef](#)]
39. Gentile, C.; Martinez, Y.; Cabrera, F. Dynamic investigation of a repaired cable-stayed bridge. *Earthq. Eng. Struct. Dyn.* **1997**, *26*, 41–59. [[CrossRef](#)]
40. Sevim, B.; Bayraktar, A.; Altunişik, A.C.; Atamtürkür, S.; Birinci, F. Assessment of nonlinear seismic performance of a restored historical arch bridge using ambient vibrations. *Nonlinear Dyn.* **2011**, *63*, 755–770. [[CrossRef](#)]
41. Li, B.; Duffield, C.F.; Hutchinson, G.L. The influence of non-structural components on the serviceability performance of high-rise buildings. *Aust. J. Struct. Eng.* **2009**, *10*, 53–62. [[CrossRef](#)]
42. Ewins, D.J. *Modal Testing: Theory, Practice and Application*; John Wiley & Sons: Hoboken, NJ, USA, 2009.
43. Jacobsen, N.J.; Andersen, P.; Brincker, R. Using Enhanced Frequency Domain Decomposition as a Robust Technique to Harmonic Excitation in Operational Modal Analysis. In Proceedings of the ISMA2006: International Conference on Noise & Vibration Engineering, Leuven, Belgium, 18 September 2006; Katholieke Universiteit: Leuven, Belgium, 2006.
44. Türker, T.; Kartal, M.E.; Bayraktar, A.; Muvafik, M. Assessment of semi-rigid connections in steel structures by modal testing. *J. Constr. Steel Res.* **2009**, *65*, 1538–1547. [[CrossRef](#)]
45. Brincker, R.; Zhang, L.; Andersen, P. Modal Identification from Ambient Responses Using Frequency Domain Decomposition. In Proceedings of the 18th International Modal Analysis Conference (IMAC), San Antonio, TX, USA, 7 February 2000.
46. Peeters, B.; De Roeck, G. Stochastic system identification for operational modal analysis: A review. *J. Dyn. Syst. Meas. Control* **2001**, *123*, 659–667. [[CrossRef](#)]
47. Extractor, A. *Structural Vibration Solutions*; Aalborg University: Aalborg, Denmark, 1999.
48. AS 4100:1998; AS, Steel Structures. Standards Australia: Sydney, Australia, 1998.
49. AS/NZS 1170.2; Structural Design Actions, Part 2: Wind Actions. Standards Australia: Sydney, Australia, 2011.
50. Brincker, R.; Zhang, L.; Andersen, P. Output-Only Modal Analysis by Frequency Domain Decomposition. In Proceedings of the ISMA25: 2000 International Conference on Noise and Vibration Engineering, Leuven, Belgium, 13 September 2000; Katholieke Universiteit: Leuven, Belgium, 2000.